Accepted Manuscript

Fixed and mobile-bearing total ankle prostheses: Effect on tibial bone strain

Alexandre Terrier, Caroline Sieger Fernandes, Maïka Guillemin, Xavier Crevoisier

Please cite this article as: Alexandre Terrier, Caroline Sieger Fernandes, Maïka Guillemin, Xavier Crevoisier , Fixed and mobile-bearing total ankle prostheses: Effect on tibial bone strain, *Clinical Biomechanics* (2017), doi: 10.1016/j.clinbiomech.2017.07.009

Fixed and Mobile-Bearing Total Ankle Prostheses: Effect on Tibial Bone Strain

Terrier, Alexandre (PhD)[1]; Fernandes, Caroline Sieger (MSc)[1]; Guillemin, Maïka (MSc)[1]; Crevoisier, Xavier (MD)[2]

1) Laboratory of Biomechanical Orthopedics
   Ecole Polytechnique Fédérale de Lausanne
   Station 19
   1015 Lausanne
   Switzerland

2) Service of Orthopaedics and Traumatology
   University Hospital Center and University of Lausanne
   Rue du Bugnon 46
   1011 Lausanne
   Switzerland

Corresponding author:
Alexandre Terrier, PhD
Laboratory of Biomechanical Orthopedics
Ecole Polytechnique Fédérale de Lausanne
Station 19
1015 Lausanne
Switzerland
Email: alexandre.terrier@epfl.ch

Word count abstract: 236 (< 250 words)
Word count main text: 3586 (< 4000 words)

Abstract

Background Total ankle replacement is associated to a high revision rate. To improve implant survival, the potential advantage of prostheses with fixed bearing compared to mobile bearing is unclear. The objective of this study was to test the hypothesis that fixed and mobile bearing prostheses are associated with different biomechanical quantities typically associated to implant failure.

Methods With a validated finite element model, we compared three cases: a prosthesis with a fixed bearing, a prosthesis with a mobile bearing in a centered position, and a prosthesis with mobile bearing in an eccentric position. Both prostheses were obtained from the same manufacturer. They were tested on seven tibias with maximum axial compression force during walking. We tested the hypothesis that there was a difference of bone strain, bone-implant interfacial stress, and bone support between the three cases. We also evaluated, for the three cases, the correlations between bone support, bone strain and bone-implant interfacial stress.

Findings There were no statistically significant differences between the three cases. Overall, bone support was mainly trabecular, and less effective in the posterior side. Bone strain and bone-implant interfacial stress were strongly correlated to bone support.

Interpretations Even if slight differences are observed between fixed and mobile bearing, it is not enough to put forward the superiority of one of these implants regarding their reaction to axial compression. When associated to the published clinical results, our study provides no argument to warn surgeons against the use of two-components fixed bearing implants.

Introduction

Total ankle replacement (TAR) is an alternative to arthrodesis for surgical treatment of end-stage arthritis. However, the implant survival rates are not as good as those being achieved for total hip (THR) or knee arthroplasty (TKR), and TAR is associated with high complication and revision rates. In a systematic review of all published annual reports of national joint registers as well as of the literature Labek et al. (Labek et al. 2011) compared the revision rates after THR, TKR and TAR respectively. They reported rates of revision per 100 observed component years to be 1.29 for THR, 1.26 for TKR and 3.29 for TAR. Cumulatively seen this corresponds to revision rates that are slightly higher than 10% after 10 years for THR and TKR, whereas revision surgery is expected by approximately one-third of all TAR patients after 10 years (Fevang et al. 2007; Besse et al. 2009; Easley et al. 2011; Labek et al. 2011; Brunner et al. 2013; Zaidi et al. 2013). Factors that can lead to this high TAR revision rate include patient's selection, surgical technique, learning curve, and implants characteristics (Henricson et al. 2007; Jonck and Myerson 2012). Main implants features that potentially play a role in the longevity of the TAR include the implant-bone interface, the amount of bone to be resected, and the level of constrained motion (Gougoulias et al. 2009). To date there is no definitive evidence of the superiority of any of the modern generation implants over the others (Jonck and Myerson 2012).

One of the questions related to the technical characteristics of the implants is to determine whether fixed or mobile bearing implants should be preferred. Worldwide the majority of implanted TARs are mobile bearing three-components designs whereas, in the USA,

almost all used TARs are fixed bearing two-components implants (Easley et al. 2011). At the moment, there are no clear reported clinical advantages of one over the other (Daniels et al. 2014; Gaudot et al. 2014; Roukis and Elliott 2015), even if a tendency towards lower revision rates associated with fixed bearing implants has been identified (Gaudot et al. 2014; Roukis and Elliott 2015). The comparative analysis of these two prostheses has not yet been addressed by finite element modeling. Besides, most current finite element models of TAR are limited to the intra-articular aspects or to the prosthetic components and there is a lack of information regarding data at the bone-implant interface (Anderson et al. 2006; Reggiani et al. 2006; Anderson et al. 2010; Espinosa et al. 2010). Intuitively, since in the fixed bearing prostheses the polyethylene and the tibial insert form a single unit, the distal tibia is subjected to higher constraints.

Therefore, the first objective of this study was to compare bone strain, bone-implant interfacial stress, and bone support, between a fixed and a mobile bearing ankle prosthesis. As a second objective, we evaluated patient variability, by analyzing the dependency of bone strain and interfacial stress on bone quality and bone support. We decided to focus our study on the Salto mobile bearing and Salto Talaris fixed bearing prostheses (Wright Medical Technology, Inc. Memphis, TN, USA) for the following reasons: 1) Both implants are produced by the same manufacturer; 2) The last author is familiar with the implantation of both prostheses. The analyses were performed with validated finite element models.

Methods

We compared three cases: a fixed bearing prosthesis (FC), a mobile bearing prosthesis
with the insert in a centered position (MC), and a mobile bearing prosthesis with the
insert in an eccentric position (ME).

A comparative analysis was performed on seven finite element models, built and
validated from seven cadaveric tibias (Terrier et al. 2014). All tibias were segmented
from CT images, using the imaging software Amira (FEI Visualization Sciences Group,
Bordeaux, France). Trabecular and cortical bone were segmented separately. Geometric
models were built using Geomagic software (Geomagic, Research Triangle Park, NC).
We virtually inserted into the seven tibia models a mobile prosthesis (Salto, Wright
Medical Technology, Inc. Memphis, TN, USA), and a fixed prosthesis (Salto Talaris,
Wright Medical Technology, Inc. Memphis, TN, USA), which is an evolution of the
mobile version. These two prostheses have nearly the same design, and are both
uncemented. However, the tibial baseplate of the fixed bearing prosthesis is more
anatomical, thicker, has a shorter cylinder at the top of the blade in order to avoid any
contact with the posterior tibial cortex, and the border to avoid bone-polyethylene contact
on the medial side of the mobile implant has been abandoned since the fixed implant does
not allow for any possibility that the polyethylene will move under the tibial plate and
come into contact with the surrounding bone (Fig. 1). The prostheses positioning and
bone cuts were done with CAD software Solidworks (Dassault Systems Simulia Corp.,
Providence, RI, USA) according to manufacturer recommendations and under the

6

supervision of an experienced foot surgeon. Prosthetic sizes were chosen to match the

tibial anatomy. The CAD models of the prostheses were obtained from the manufacturer.

In the finite element models, bone was linear elastic and non-homogeneous. Poisson's

ratio was 0.3 and the elastic Young's modulus was estimated from the Hounsfield

number of CT images of the cadaveric tibias (Keller 1994). The tibial and talus metallic

(CrCo) components were linear elastic with Poisson's ratio of 0.3 and Young's Modulus

of 210 GPa. The polyethylene (UHMWPE) components were linear elastic with

Poisson's ratio of 0.3 and Young's Modulus of 900 MPa. The contact between the tibial

implant and the tibial bone was assumed fully bonded. The contact between the tibial

implant and the polyethylene component was bounded for the fixed bearing, but also for

the mobile one, since we imposed its position. The contact between the polyethylene

component and the metallic talus implant was assumed frictionless.

We simulated maximum loading during stance phase of walking, and thus assumed an

angle of flexion of 0 degrees (Leszko et al. 2008). The loading conditions were derived

from the ASTM F2665 protocol (2014). The proximal part of the tibia was fully

constrained. A point corresponding to the rotation center of the prosthesis was rigidly

linked to the talus component. The three rotations of this point were constrained to zero,

while the translations were free. According to the ASTM protocol, an axial compressive

force of 5560 N (five times the body weight of an overweight patient) was applied on this

point for the FC and MC case. For the ME case, we considered an extreme anterior

displacement of 3.7 mm of the mobile bearing, which was estimated from in vivo

measurements (Leszko et al. 2008; Cenni et al. 2013) and also in accordance with the reported increased laxity after total ankle replacement (Watanabe et al. 2009). For the ME case, the axial loading was thus also displaced anteriorly.

The octahedral shear strain invariant was evaluated within the tibial bone (Nagaraja et al. 2005; Kettenberger et al. 2015). Within the manuscript, strain always refer to this invariant. A value of 1% was considered as critical for bone micro-damage (Carter et al. 1981; Morgan and Keaveny 2001). We thus considered the amount of total bone volume with a strain above 1%. To account for the variable size of the tibias and implants, we normalized this critical volume to the implant volume. This critical volume evaluation was performed separately for trabecular, cortical, and whole bone. Strain was also evaluated along a line 1 mm above the implant fixation blade in the sagittal plane (symmetric plane of the implant).

The interfacial shear stress was evaluated at the boundary between the tibial implant and the tibial bone. At this interface, we measured the surface area with an interfacial shear stress above 3 MPa, and normalized by the surface area of the implant in contact with the bone. A critical value of 3 MPa was considered as prone to failure (Berzins et al. 1997). This was performed separately for cortical and trabecular bone.

Since the fixed and mobile tibial implants have a slightly different design, we quantified for each tibia the bone support of the two tibial implants. We considered anterior, middle,

and posterior rectangular zones of equal size at the tibial cut, aligned with the implant. Ignoring the implant keel, we measured in each zone, the surface area of the trabecular, cortical bone, and implant. Bone support was evaluated as the percent of the total implant surface supported by trabecular and cortical bone in the anterior and posterior zones (Fig. 2). We also evaluated the percent of unsupported implant.

To account for subject variability, we evaluated the bone quality of each tibia within a specific region above the tibial implant. This volume of interest was defined as a slice of bone from the horizontal tibial resection plane up to 2 cm above the implant keel. From the CT images, we quantified the average bone density within this volume of trabecular, cortical, and whole bone. The bone density was evaluated from the Hounsfield values of the CT images.

The model was implemented in Abaqus (Dassault Systems Simulia Corp., Providence, RI, USA). The analysis was performed with the implicit solver. Bone, metallic implants and polyethylene components were meshed with quadratic tetrahedral elements. Each model contained about 650,000 degrees of freedom. The relative effect of the finite element mesh on the bone strain was less than 2%.

For statistical analysis, results data were checked for normality using a Lilliefors test. A one-way ANOVA (or Kruskal-Wallis for non-normal cases) was used to compare the FC, MC, and ME cases in terms of bone strain, bone-interface stress, and bone support. We

evaluated linear correlations between the normalized critical bone volume and the

trabecular, cortical, and whole bone. For the bone-implant interfacial stress, we evaluated

the correlations with bone density, and bone support. The linear Pearson coefficient of

determination (R^2) and the associated p value were calculated for each correlation tested.

The statistical analysis was performed with Matlab (The Mathworks, Inc., Natick, MA,

USA).

Results

Bone strain was highest around the cylindrical part of the blade, at the anterior and posterior edges, for the seven tibias and the three cases (Fig. 3). The strain along a posterior-anterior line 1 mm above the cylindrical part of the implant produced a similar pattern for all tibias: two peaks and a plateau in between. Compared to FC, MC showed no difference, while ME had increased bone strain on the anterior side. Among all simulated cases, the normalized critical bone (cortical and trabecular) strain volume varied from 3% to 188% (Fig. 4). There were no significant ($p > 0.36$) differences of critical volume between the three cases.

The interfacial stress peak was located above the keel and at the plate rim (Fig. 5). There was a greater surface of critical interfacial stress in the trabecular bone (8.4% on average) compared to the cortical bone (0.3% on average). The overall (total) surface of critical interfacial stress varied from 5.2% to 13.3% (Fig. 6). There were no significant ($p > 0.63$) differences of critical surface of interfacial stress between the three cases.

Bone support of the fixed implant was provided at 93.0% by trabecular bone and 6.1% by cortical bone, while 0.9% was unsupported. Bone support of the mobile implant was provided at 94.7% by the trabecular bone and 4.8% by the cortical bone, while 0.5% was unsupported. Bone support was higher in the anterior zone, for the fixed (33.5%) and mobile (33.8%) prostheses, and both implants had a lower posterior support (25.2%).

11

There was no statistical difference between the fixed implant and the mobile implant in terms of support ($p > 0.05$).

The relative volume of critical strain in trabecular bone was strongly (negatively) correlated to bone quality, especially to the quality of trabecular bone (Table 1). This correlation was not present for cortical bone strain. The relative surface of critical interfacial stress was also strongly correlated to trabecular bone strain, to a lower extent. Among all combinations of bone support (anterior/posterior, trabecular/cortical/none), only the lack of anterior support was (positively) linearly correlated ($R^2 = 0.62$, $p < 0.0001$) to cortical bone strain, and the lack of posterior bone support was (positively) correlated ($R^2 = 0.36$, $p = 0.004$) to trabecular strain. The correlation between interfacial stress and bone support was significant, especially at the cortical bone interface, and was associated to trabecular bone support ($R^2 = 0.59$, $p < 0.0001$) and cortical bone support ($R^2 = 0.57$, $p = 0.0001$).

Discussion

To our knowledge only two studies exist comparing the clinical results of the Salto

mobile bearing and the Salto Talaris fixed bearing prostheses. The first one is a

multicenter retrospective comparative study of 33 Salto versus 33 pared Salto Talaris

with a mean follow up of two years (Gaudot, Colombier et al., 2014). No significant

differences in terms of clinical performance were observed. However, radiographic

analysis of the distal tibia revealed a higher proportion of radiolucent lines, decrease of

the trabecular density around the keel, and subchondral cysts in the Salto mobile patients.

Despite this radiographic findings the authors concluded that longer follow-up is

necessary to establish definitive recommendations. The second study conducted by

Roukis and Eliott (Roukis and Elliott 2015) is a systematic review of the revision

incidence following primary implantation of the Salto mobile bearing and the Salto

Talaris fixed bearing prostheses. Reviewed studies included 1209 Salto mobile and 212

Salto Talaris prostheses with a weighted mean follow up of almost three years. The

revision rate was 50% lower in the Salto Talaris group but no obvious difference in the

etiology for revision could be identified. Beside the two studies strictly comparing the

Salto mobile and the Salto Talaris prostheses we are aware of a single clinical report

focusing on the fixed-bearing versus mobile-bearing question (Queen et al. 2014). In their

therapeutic level II trial Queen et al. compare patient-reported outcome, function, and

gait mechanics in two groups of 40 patients in whom either a Salto Talaris fixed bearing

or a Scandinavian Total Ankle Replacement (STAR) mobile bearing prosthesis was

implanted. The Salto Talaris was shown to perform biomechanically better while the

STAR mobile bearing was associated with better results regarding patient-reported pain

outcome. In summary, today, there is no rational to clinically establish the superiority of a fixed bearing over a mobile bearing type of prosthesis for total ankle replacement.

Using a validated finite element model (Terrier et al. 2014), we compared both Salto mobile bearing and Salto Talaris fixed bearing prosthesis types. Based on seven tibias, our results showed that there are no significant differences in critical bone strain and bone-implant interface stress between the two prostheses. However, we observed a strong correlation of these two quantities with bone quality. Bone support was comparable for both prostheses.

Although we were able to test our hypothesis on seven tibias, we were still limited here by a single and simplified loading. We might indeed observe other stress and strain patterns for more complex loading. However, very few models are using more complex loading (Arnold et al. 2010; Leardini et al. 2014; Wang et al. 2016; DeMers et al. 2017), and the comparison with our results remains difficult since bone strain is rarely analyzed (Reggiani et al. 2006; Jay Elliot et al. 2014). Besides, since we had no information about the donor, we applied the same loading to all tibias, which is certainly not fully consistent with real life. The eccentric case simulated here covered reported extreme displacements of the mobile bearing (Siegler et al. 2005; Reggiani et al. 2006; Leszko et al. 2008). However, the loading conditions used here correspond to an extreme worst case loading, and should therefore be representative of the potential mechanical effects that might lead to failure in these two types of prostheses. We used a specific prosthesis, with a mobile and fixed bearing version, but we assume reasonable that the conclusions would be the

14

same for another prosthesis. We used a critical strain value of 1% as an estimate of bone

damaging strain (Carter et al. 1981; Morgan and Keaveny 2001). The critical value of

interfacial stress of 3 MPa was also reported as initiation of bone-implant bonding failure

(Berzins et al. 1997). This critical interfacial stress value was estimated for trabecular

bone, but used here for both trabecular and cortical bone. While we may expect a

different value for cortical bone, we assume that this simplification had a slight effect

since shear stress mainly occurred at the trabecular interface. Even if these values were

approximate, they would not change our conclusions. The strength of this study is to

compare the same three cases on seven validated finite element models of the distal tibia

with a tibial component. By using a validated finite element model of the tibial

component, we were able to statistically quantify the difference between a fixed and a

mobile prosthesis on seven specific tibias. The fact that our testing only includes the

tibial component may appear as a limitation. However, the difference between the

designs of the assessed prostheses concerns the tibial part only.

The predicted strain was consistent with the reported value of 0.3% (3000 microstrains)

for typical activities (Yang et al. 2011; Al Nazer et al. 2012). The predicted strain within

tibial bone exceeded this limit around the implant keel, for all tibias. The loading

considered here was however extreme. The predicted strains suggest that bone micro-

damage might occur around the blade and at the border of the plate (Al Nazer et al.

2012). This is also consistent with the prediction of bone-implant interfacial stress, which

were located around the keel and at the rim of the plate. These are typical location for

reported radiological bone densification as it has been measured using bone mineral

densitometry (Zerahn et al. 2000). Furthermore, in a finite element model calculation, an increased bone density was expected above the anchoring bolts (Bouguecha et al. 2011). Although the fixed and mobile designs have a different shape of the baseplate, it was not associated to a difference of bone support. Among the three tested mechanical quantities in this biomechanical comparison, none showed an advantage of the mobile on the fixed prosthesis.

The observed strong correlation between bone strain and bone quality is reasonable, and confirms the importance of modeling specifically the bone quality of the patient. More precisely, the results showed the importance of the trabecular bone. In fact, this is logically understandable because, due to the particular anatomical shape of the distal tibia, there are only few cortical portions which support the tibial component of the prosthesis. Even if custom-made implants (based on 3D CT scan planning) were used, the cortical support would remain low, and high constraints would still be transmitted to the trabecular bone.

The methodology presented here with cadaveric tibia should be applied retrospectively on real patients. Using (quantitative) CT, patient weight and height, along with kinematics data, we expect a good estimation of bone strain state of the patient. We might thus define series of patients that could be tested for specific questions associated to prosthesis design or surgical technique. Furthermore, since a positive correlation between bone density around the prosthesis and patient's outcome has been reported (Zerahn and Kofoed 2004), our methodology, applied to real patients, may contribute to further

16

understand the role of bone density for outcome in different types of prostheses. In a next step, the method, or its results on retrospective patients, could be used preoperatively to propose optimal implants for specific patients.

The etiology for the high incidence of revision after TAR is still unclear and probably depends both upon patient and implant related factors. Regarding the latter, mechanical, i.e. implant's design, and biological, i.e. implant's coating, aspects can be taken into consideration. Understanding the respective contribution of both aspects is crucial and our model has the potential to characterize and quantify the first one.

The eccentric position of the mobile bearing slightly increased the anterior peak strain, but not significantly. We concluded that, even if slight differences are observed between fixed and mobile bearing, it is not enough to put forward the superiority of one of these implants regarding their reaction to axial compression. Nevertheless, when associating our findings to the clinical results showing a tendency to better performance of the fixed bearing Salto Talaris prostheses, we can also conclude that there is no argument to warn surgeons from using fixed bearing implants.

17

Ethical review committee statement: This study was performed on cadaveric samples,

and did not required ethical committee approval.

References

(2014). ASTM F2665-09(2014), Standard Specification for Total Ankle Replacement Prosthesis. A. International. West Conshohocken, PA.

Al Nazer, R., J. Lanovaz, et al. (2012). "Direct in vivo strain measurements in human bone-a systematic literature review." J Biomech **45**(1): 27-40.

Anderson, D. D., J. K. Goldsworthy, et al. (2006). "Intra-articular contact stress distributions at the ankle throughout stance phase-patient-specific finite element analysis as a metric of degeneration propensity." Biomechanics and Modeling in Mechanobiology **5**(2-3): 82-89.

Anderson, D. D., Y. Tochigi, et al. (2010). "Effect of implantation accuracy on ankle contact mechanics with a metallic focal resurfacing implant." J Bone Joint Surg Am **92**(6): 1490-1500.

Arnold, E. M., S. R. Ward, et al. (2010). "A model of the lower limb for analysis of human movement." Ann Biomed Eng **38**(2): 269-279.

Berzins, A., B. Shah, et al. (1997). "Nondestructive measurements of implant-bone interface shear modulus and effects of implant geometry in pull-out tests." J Biomed Mater Res **34**(3): 337-340.

Besse, J. L., N. Brito, et al. (2009). "Clinical evaluation and radiographic assessment of bone lysis of the AES total ankle replacement." Foot Ankle Int **30**(10): 964-975.

Bouguecha, A., N. Weigel, et al. (2011). "Numerical simulation of strain-adaptive bone remodelling in the ankle joint." Biomed Eng Online **10**: 58.

Brunner, S., A. Barg, et al. (2013). "The Scandinavian total ankle replacement: long-term, eleven to fifteen-year, survivorship analysis of the prosthesis in seventy-two consecutive patients." J Bone Joint Surg Am **95**(8): 711-718.

Carter, D. R., W. E. Caler, et al. (1981). "Fatigue behavior of adult cortical bone: the influence of mean strain and strain range." Acta Orthop Scand **52**(5): 481-490.

Cenni, F., A. Leardini, et al. (2013). "Functional performance of a total ankle replacement: thorough assessment by combining gait and fluoroscopic analyses." Clin Biomech (Bristol, Avon) **28**(1): 79-87.

Daniels, T. R., A. S. Younger, et al. (2014). "Intermediate-term results of total ankle replacement and ankle arthrodesis: a COFAS multicenter study." J Bone Joint Surg Am **96**(2): 135-142.

DeMers, M. S., J. L. Hicks, et al. (2017). "Preparatory co-activation of the ankle muscles may prevent ankle inversion injuries." J Biomech **52**: 17-23.

Easley, M. E., S. B. Adams, Jr., et al. (2011). "Results of total ankle arthroplasty." J Bone Joint Surg Am **93**(15): 1455-1468.

Espinosa, N., M. Walti, et al. (2010). "Misalignment of total ankle components can induce high joint contact pressures." The Journal of bone and joint surgery. American volume **92**(5): 1179-1187.

Fevang, B. T., S. A. Lie, et al. (2007). "257 ankle arthroplasties performed in Norway between 1994 and 2005." Acta Orthop **78**(5): 575-583.

Gaudot, F., J. A. Colombier, et al. (2014). "A controlled, comparative study of a fixed-bearing versus mobile-bearing ankle arthroplasty." Foot Ankle Int **35**(2): 131-140.

Gougoulias, N. E., A. Khanna, et al. (2009). "History and evolution in total ankle arthroplasty." <u>Br Med Bull</u> **89**: 111-151.

Henricson, A., A. Skoog, et al. (2007). "The Swedish Ankle Arthroplasty Register: An analysis of 531 arthroplasties between 1993 and 2005." <u>Acta Orthop</u> **78**(5): 569-574.

Jay Elliot, B., D. Gundapaneni, et al. (2014). "Finite element analysis of stress and wear characterization in total ankle replacements." <u>J Mech Behav Biomed Mater</u> **34**: 134-145.

Jonck, J. H. and M. S. Myerson (2012). "Revision total ankle replacement." <u>Foot Ankle Clin</u> **17**(4): 687-706.

Keller, T. S. (1994). "Predicting the compressive mechanical behavior of bone." <u>J Biomech</u> **27**(9): 1159-1168.

Kettenberger, U., A. Latypova, et al. (2015). "Time course of bone screw fixation following a local delivery of Zoledronate in a rat femoral model - A micro-finite element analysis." <u>J Mech Behav Biomed Mater</u> **45**(0): 22-31.

Labek, G., H. Klaus, et al. (2011). "Revision rates after total ankle arthroplasty in sample-based clinical studies and national registries." <u>Foot Ankle Int</u> **32**(8): 740-745.

Labek, G., M. Thaler, et al. (2011). "Revision rates after total joint replacement: cumulative results from worldwide joint register datasets." <u>J Bone Joint Surg Br</u> **93**(3): 293-297.

Leardini, A., J. J. O'Connor, et al. (2014). "Biomechanics of the natural, arthritic, and replaced human ankle joint." <u>J Foot Ankle Res</u> **7**(1): 8.

Leszko, F., R. D. Komistek, et al. (2008). "In vivo kinematics of the salto total ankle prosthesis." Foot Ankle Int **29**(11): 1117-1125.

Morgan, E. F. and T. M. Keaveny (2001). "Dependence of yield strain of human trabecular bone on anatomic site." J Biomech **34**(5): 569-577.

Nagaraja, S., T. L. Couse, et al. (2005). "Trabecular bone microdamage and microstructural stresses under uniaxial compression." J Biomech **38**(4): 707-716.

Queen, R. M., T. L. Sparling, et al. (2014). "Patient-Reported Outcomes, Function, and Gait Mechanics After Fixed and Mobile-Bearing Total Ankle Replacement." J Bone Joint Surg Am **96**(12): 987-993.

Reggiani, B., A. Leardini, et al. (2006). "Finite element analysis of a total ankle replacement during the stance phase of gait." J Biomech **39**(8): 1435-1443.

Roukis, T. S. and A. D. Elliott (2015). "Incidence of revision after primary implantation of the salto((R)) mobile version and salto talaris total ankle prostheses: a systematic review." J Foot Ankle Surg **54**(3): 311-319.

Siegler, S., J. K. Udupa, et al. (2005). "Mechanics of the ankle and subtalar joints revealed through a 3D quasi-static stress MRI technique." J Biomech **38**(3): 567-578.

Terrier, A., X. Larrea, et al. (2014). "Development and experimental validation of a finite element model of total ankle replacement." J Biomech **47**(3): 742-745.

Wang, Y., D. W. Wong, et al. (2016). "Computational Models of the Foot and Ankle for Pathomechanics and Clinical Applications: A Review." Ann Biomed Eng **44**(1): 213-221.

Watanabe, K., X. M. Crevoisier, et al. (2009). "Analysis of joint laxity after total ankle arthroplasty: cadaver study." Clin Biomech (Bristol, Avon) **24**(8): 655-660.

Yang, P. F., G. P. Brüggemann, et al. (2011). "What do we currently know from in vivo bone strain measurements in humans?" Journal of Musculoskeletal Neuronal Interactions **11**(1): 8-20.

Zaidi, R., S. Cro, et al. (2013). "The outcome of total ankle replacement: a systematic review and meta-analysis." Bone Joint J **95-B**(11): 1500-1507.

Zerahn, B. and H. Kofoed (2004). "Bone mineral density, gait analysis, and patient satisfaction, before and after ankle arthroplasty." Foot Ankle Int **25**(4): 208-214.

Zerahn, B., H. Kofoed, et al. (2000). "Increased bone mineral density adjacent to hydroxy-apatite-coated ankle arthroplasty." Foot Ankle Int **21**(4): 285-289.

Figure Legends

Figure 1. Three cases were compared: the Talaris fixed bearing (left), the Salto mobile bearing centered (middle), and the Salto mobile bearing anteriorly eccentered (right).

Figure 2. The bone support of the tibial implant is measured in two zones: anterior (A) and posterior (P). In this bottom-up view of the tibial cut, the cortical (red) and trabecular bone (dark green) support is measured as a percentage of the total implant surface, in each zone.

Figure 3. This sagittal cut view shows a typical example of bone strain distribution within the tibia, and along a (white dotted) line above the implant keel. Bone strain was maximal around the implant keel. Compared to the fixed implant (left), the strain was shifted anteriorly with the anterior eccentric mobile component (right).

Figure 4. Boxplot of the volume of bone strain above the critical value of 1% normalized by the implant volume. The edges of the box are the 25th and 75th percentiles and the whiskers extend to the most extreme data points. The median values are shown as a line across the box and the mean values are depicted as a circle.

Figure 5. This bottom-up view of a typical example represents the distribution of bone-implant interfacial shear stress. Critical (red) stress are located around the keel and at the rim of the plate. The mobile eccentric case display slightly more interfacial stress.

Figure 6. Boxplot of the area of interfacial stress above the critical value of 3 MPa normalized by the implant surface area for the three cases. The edges of the box are the 25th and 75th percentiles and the whiskers extend to the most extreme data points. The median values are shown as a line across the box and the mean values are depicted as a circle.

Table 1. Correlation between (cortical and trabecular) bone density and volume of critical (cortical and trabecular) bone strain, and critical surface of (cortical and trabecular) bone-implant interfacial stress.

Fixed Centered | Mobile Centered | Mobile Eccentric
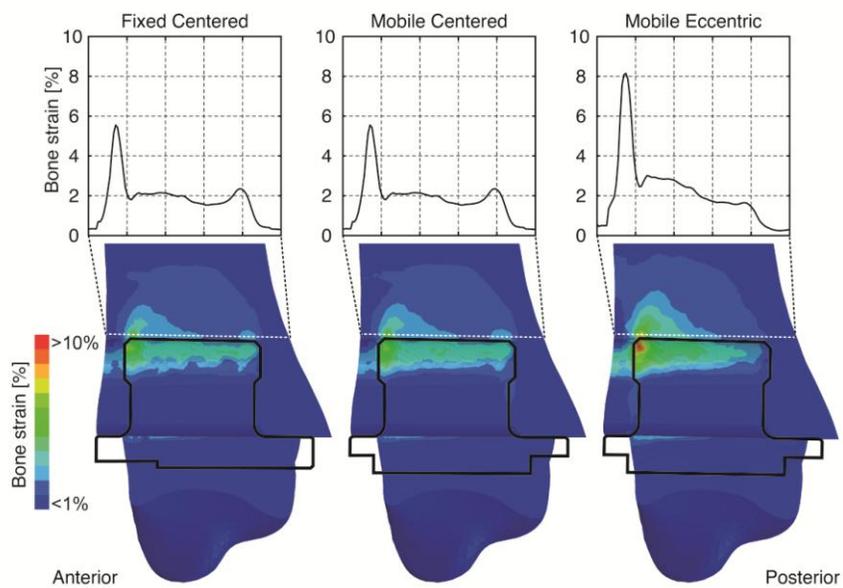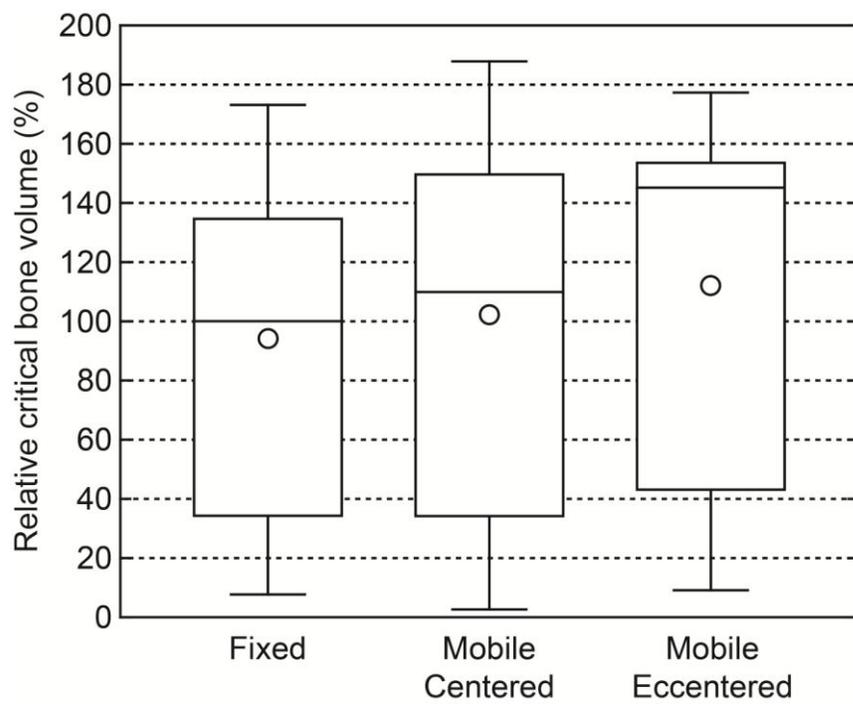
3.7 mm
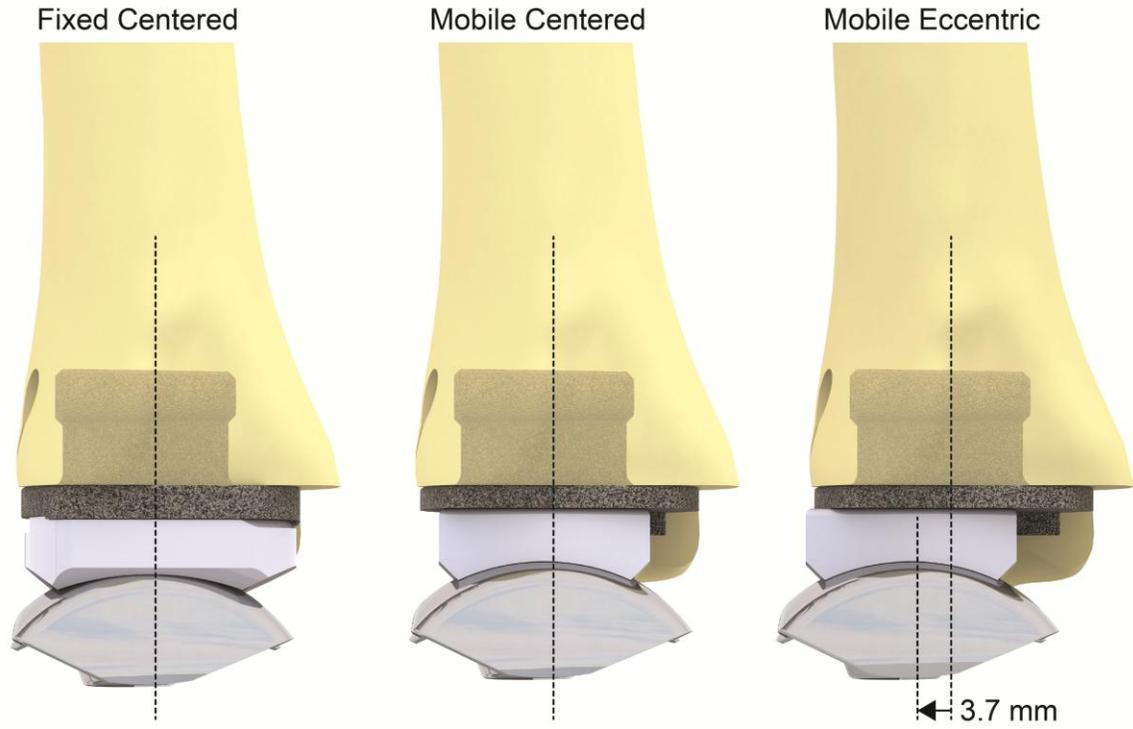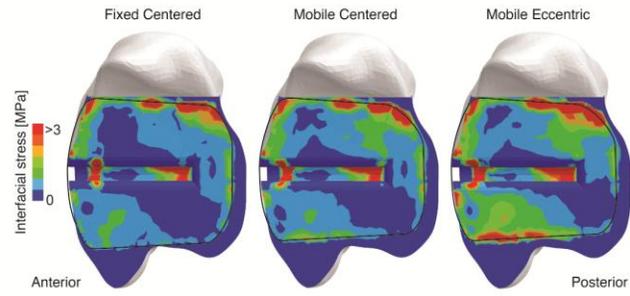
Figure 1

Figure 2

Figure 3

Figure 4

Figure 5
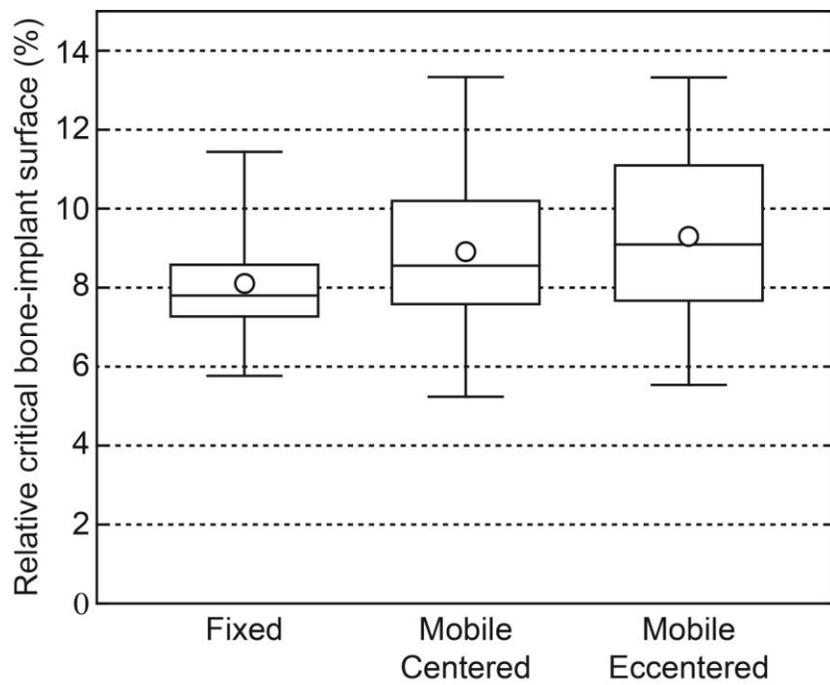
Figure 6

Table 1

		Bone density			
		Trabecular		Cortical	
		R^2	p	R^2	p
Bone Strain	**Trabecular**	0.9086	2.54E-11	0.5621	0.0001
	Cortical	0.1649	0.0678	0.1848	0.0518
Interfacial Stress	**Trabecular**	0.5663	0.0001	0.0784	0.2189
	Cortical	0.2399	0.0242	0.0429	0.3679

Highlights
- Finite element analysis of ankle arthroplasty to compare fixed and mobile insert
- No significant (n=7) differences in bone strain
- Strong correlation between bone strain and bone support